Oxygenated heterocyclic metabolites with dual cyclooxygenase-2 and 5-lipoxygenase inhibitory potentials from Rhizophora annamalayana

Kajal Chakraborty & Vamshi Krishna Raola

Medicinal Chemistry Research

ISSN 1054-2523
Volume 27
Number 6

Med Chem Res (2018) 27:1679-1689
DOI 10.1007/s00044-018-2182-0

Medicinal Chemistry Research (2018) 27:1679–1689
https://doi.org/10.1007/s00044-018-2182-0

MEDICINAL CHEMISTRY RESEARCH

ORIGINAL RESEARCH

Oxygenated heterocyclic metabolites with dual cyclooxygenase-2 and 5-lipoxygenase inhibitory potentials from *Rhizophora annamalayana*

Kajal Chakraborty[1] · **Vamshi Krishna Raola**[1,2]

Received: 25 December 2017 / Accepted: 16 April 2018 / Published online: 4 May 2018

Abstract

Previously undescribed oxygenated heterocyclic metabolites were purified from the ethyl acetate fraction of natural mangrove hybrid *Rhizophora annamalayana*. The purified metabolites were characterized as 11-(tetrahydro-14α-hydroxy-13β-methylfuran-12-yl)-10β-methylbutyl benzoate (**1**), 13-(tetrahydro-15β,16α-dimethyl-18-oxo-2*H*-pyran-14-yl)-10β-methylhept-12(*E*)-enyl benzoate (**2**), and dihydro-11-((7*E*)-2-hydroxy-8β-methyl-2*H*-chromen-9-yl)-13-methylpent-12(*E*)-enyl)-17β-methylfuran-19(3*H*)-one (**3**) by the combined spectroscopic experiments. These metabolites were assessed for their antioxidant and anti-inflammatory activities, and compared with the commercially available standards. The purified compound **3** exhibited greater antioxidant activities as deduced by 2, 2'-azino-bis(3-ethylbenzothiazoline-6-sulfonic acid and 2, 2-diphenyl-1-picrylhydrazyl quenching properties (IC_{50} 2.10 and 2.22 mM, respectively) compared to the positive control (*α*-tocopherol, IC_{50} 1.46 and 1.69 mM, respectively). Consequently, the anti-inflammatory activity of compound **3** with regard to the inhibitory property towards pro-inflammatory 5-lipoxygenase was greater (IC_{50} 2.16 mM) than that exhibited by the synthetic anti-inflammatory drug ibuprofen (IC_{50} 4.51 mM). Electronic and hydrophobic parameters were deduced to find the target bioactivities of the studied compounds. These oxygenated heterocyclic metabolites could be used as potential therapeutic lead compounds in the pharmaceutical applications.

Keywords *Rhizophora annamalayana* · Rhizophoraceae · Natural hybrid mangrove · Oxygenated heterocyclic metabolites · Antioxidative · Anti-inflammatory

Introduction

Rhizophora annamalayana (Kathir) is a relatively recently characterized mangrove species (Kathiresan 1999) as compared to other members of the family Rhizophoraceae. This species is a natural hybrid derived from *R. apiculata* and *R. mucronata*, which are perennial mangroves, endemic to the Southeast Asia (Kathiresan 1999; Parani et al. 1997; Lakshmi et al. 2002). *R. annamalayana* is a unique mangrove hybrid species found in Southeast Asia, predominantly in peninsular India, and the Nicobar Islands of the Bay of Bengal (Kathiresan 1999; Ragavan et al. 2015). Several species of genus *Rhizophora* are widely used in the traditional medicines to treat inflammation, diabetes, and rheumatism (Kusuma et al. 2011). Fewer earlier reports of literature described the phytochemical studies and secondary metabolites of *R. annamalayana* (Alikunhi et al. 2012; Moovendhan et al. 2015; Chakraborty and Raola 2018; Raola and Chakraborty 2017a, 2017b). Mangrove plants have morphologically adapted structures and their specialized physiological mechanisms help them survive in an oxygen deficient soil conditions and higher salinity ecosystems. These specialized adaptations were reported to enable these mangrove plants to biosynthesis various biologically active metabolites to sustain their adverse living

Electronic supplementary material The online version of this article (https://doi.org/10.1007/s00044-018-2182-0) contains supplementary material, which is available to authorized users.

✉ Kajal Chakraborty
kajal_cmfri@yahoo.com
kajal.chakraborty@icar.gov.in

[1] Marine Bioprospecting Section of Marine Biotechnology Division, Central Marine Fisheries Research Institute, Ernakulam North P. O., P.B. No. 1603, Cochin, India

[2] Department of Chemistry, Mangalore University, Mangalagangothri, Mangalore, Karnataka State 574199, India

conditions (Nebula et al. 2013). Earlier investigations on the chemical compounds from mangrove species, especially those belonging to the family Rhizophoraceae, identified the occurrence of bioactive metabolites with diverse structural frameworks, such as tannins, saponins, triterpenoids, alkaloids, polyketides, flavonoids, steroids, aryl terpenoids, pimaranes, labdanes, chromenes, and kauranes (Wang et al. 2004; Wang et al. 2005; Rohini and Das 2010; Nebula et al. 2013; Costa et al. 2014; Laskar and Brahmachari 2014; Jameel et al. 2015; Chakraborty and Raola 2017; Martins et al. 2017; Raola and Chakraborty 2017a), which were endowed with potent chemical and biological activities (Rocha-Santos and Duarte 2014; Hegazy et al. 2015).

As a part of the ongoing search to characterize biologically active metabolites of medicinal significance from different species of mangrove plants, we have considered the natural mangrove hybrid *R. annamalayana* (Kathir) in the present study. An earlier report of literature described the anti-inflammatory properties of the crude extracts obtained from *R. annamalayana* (Alikunhi et al. 2012). However, very limited studies were attempted to characterize the bioactive compounds responsible for pharmacological properties (Raola and Chakraborty 2017b; Chakraborty and Raola 2018). The present study aimed to evaluate the isolation and structural elucidation of the hitherto undescribed oxygenated heterocyclic metabolites from the ethyl acetate (EtOAc) fraction of *R. annamalayana* by comprehensive spectral analysis. Their anti-inflammatory potentials were determined by in vitro inhibitory properties towards pro-inflammatory cyclooxygenase (COX-1 and 2) and lipoxygenase (5-LOX) assays, whereas the antioxidative activities were evaluated by their scavenging capacities of the free radicals {1, 1-diphenyl-2-picrylhydrazyl ($DPPH^{\cdot}$) and 2, 2′-azino-bis-3 ethylbenzothiozoline-6-sulfonic acid diammonium salt ($ABTS^{\cdot+}$)}. Quantitative structure–activity relationship analyses to understand the structural parameters, which have been responsible for target bioactivities, were described. This is the first report of oxygenated heterocyclic metabolites with dual cyclooxygenase-2 and 5-lipoxygenase inhibitory potentials from *R. annamalayana*.

Materials and methods

General experimental procedures

The infra-red (IR) spectral data were acquired by using a Perkin–Elmer model 2000 Fourier-transform infrared (FTIR) instrument scanning between 4000 to 400 cm^{-1} by preparing potassium bromide (KBr) pellets. The UV (ultraviolet) spectra were obtained on a spectrometer (Varian Cary 50, USA). Mass chromatograms were obtained by using a gas chromatograph (Varian GC, CP-3800) executed in an electronic impact (EI) mode. Proton and carbon nuclear magnetic resonance (NMR) spectra (^{1}H and ^{13}C NMR) along with two-dimensional (2D) NMR, such as heteronuclear multiple bond correlation (HMBC), nuclear overhauser effect spectroscopy (NOESY), heteronuclear single quantum coherence (HSQC), and ^{1}H-^{1}H correlated spectroscopy (COSY) were extracted on the Bruker Avance DPX (500 MHz) with trimethylsilyl hydride (Me_3SiH) as an internal standard. Mass spectral data were acquired on a Perkin–Elmer Q-Tof-Mass Spectrometer (Clarus 680). The purified compounds were analyzed for homogeneity on an high performance liquid chromatography (HPLC) (Model Shimadzu LC 20AD, Japan) instrument coupled with binary gradient pump (Shimadzu LC 2535) bound with C_{18} column (Phenomenex USA, Luna® 5 µm C_{18} 100 Å, LC column 250 × 4.6 mm) linked to photodiode array detector. Analytical grade chemicals and solvents used in this study were purchased from the Sigma Aldrich (Missouri, USA) and E-Merck (Darmstadt, Germany), whichever appropriate.

Plant material

The freshly available leaves of *R. annamalayana* (order Malpighiales, family Rhizophoraceae) were harvested from Pichavaram, Tamil Nadu region located between 11°20' to 11°30' north (latitude) and 79°45' to 79°55' east (longitude) along with South-eastern coast of the Indian peninsula. The collected plant leaves (~ 1.25 kg) were rigorously cleaned in running water and kept for shade drying (33 ± 2°C, 48 h).

Extraction and isolation

The shade-dried leaf materials were ground to fineness (0.48 kg) before being extracted with an aqueous methanol (H_2O: MeOH 1:4 v/v) at 45–60 °C for 4 h. The collected extract was concentrated to one-third volume in vacuo (at 50 °C) with a rotary evaporator to yield crude methanol extract. The crude aqueous methanol extract was partitioned with ethyl acetate (EtOAc, 150 mL X 3) and concentrated in vacuo (at 50 °C) with a rotary evaporator (Heidolph, Germany) to yield the EtOAc fraction (24 g). A portion of the EtOAc fraction (21 g) was initially mixed with the silica gel (5 g, 60–120 meshed), before being submitted to vacuüm chromatography, on a glass column (900 × 40 mm) filled with coarse silica gel (60–120 meshed, 0.06 kg). An initial elution with *n*-hexane eliminated the waxy material, and the mobile phase polarity was increased by adding EtOAc (0–30% EtOAc in *n*-hexane) to yield a total of 16 sub-fractions (20 mL each), which were combined to six groups (RA_1-RA_6) based on TLC experiments (at *n*-hexane: EtOAc, 4:1 v/v). Among different fractions, RA_2, RA_4, and RA_6 displayed greater activities, and therefore, were selected for further purification. The fraction RA_2 (514.3 mg, collected at 4% EtOAc in *n*-hexane) was flash fractionated

(BiotageAB, Sweden, 230–400 mesh) with mobile phase EtOAc/*n*-hexane (0–10% EtOAc) to yield 90 sub-fractions (8 mL each). These sub-fractions were combined to eight-derived fractions (72 mL, $RA_{21}-RA_{28}$) after TLC (*n*-hexane: EtOAc, 4:1, v/v) and HPLC (MeOH: ACN, 1:4 v/v) experiments. Among the active fractions, RA_{23} (215 mg) was sub-fractionated over a semi-preparative gradient reverse-phase (RP) HPLC {with MeOH/ACN (8:17 through 32:23 v/v) mobile phase} on a bonded phase C_{18} column, which was serially connected with a diode array detector to yield **1** (126.8 mg) as pure compound. The homogeneity of **1** was determined by the TLC (with 10% EtOAc/*n*-hexane) and RP-HPLC (MeOH: ACN, 1:4 v/v) experiments. Further, the bioactive fraction RA_4 (456 mg) was flash fractionated on 230–400 meshed silica gel with mobile phase 0–60% EtOAc/*n*-hexane and 0–12% MeOH/$CHCl_3$ to yield eighty sub-fractions (8 mL each). These sub-fractions were combined to eight-derived fractions (RA_{41}-RA_{48}) after TLC (*n*-hexane: EtOAc, 4:1, v/v) and HPLC (MeOH: ACN, 1:4 v/v) experiments. The fraction RA_{46} (96 mg) was sub-fractionated over a semi-preparative RP-C_{18} bound to HPLC (with solvent MeOH/ACN, 2:3 v/v) to yield **2** (52.5 mg) as a pure compound. The homogeneity was ascertained by TLC (with 20% EtOAc/*n*-hexane) and RP-HPLC (MeOH: ACN, 2:3 v/v). Likewise, the fraction RA_6 (287 mg) was separated by flash chromatography (with 0–90% EtOAc/*n*-hexane and later with 20% MeOH/$CHCl_3$) to yield a total of 62 sub-fractions (9 mL each), which were combined to six-derived fractions (RA_{61}–RA_{66}). The fraction RA_{65} (107 mg) was found to be active, and therefore, was selected for further fractionation over semi-preparative RP-C_{18} HPLC with stepwise gradient of ACN and water (ACN: water, 1:4 through 1:1, v/v) to yield **3** (81.4 mg), which was found to be homogeneous after TLC (15% MeOH/$CHCl_3$) and HPLC (MeOH: ACN, 1:1 v/v).

11-(Tetrahydro-14α-hydroxy-13β-methylfuran-12-yl)-10β-methylbutyl benzoate (1)

Pale yellow liquid, UV_{MeOH} λ_{max}: 237 nm (log ε 3.40); TLC (EtOAc/*n*-hexane 1:9 v/v) R_f: 0.85; RP-HPLC (MeOH: ACN, 3:7 v/v) R_t: 18.56 min; IR (KBr; ν = stretching, δ = bending, ρ = rocking vibrations) ν_{max} in cm^{-1}: 721.4 (mono-subst –C–H δ), 805.31 (aryl C–H δ), 1378.18 (C–H ρ), 1457.27 (C = C ν), 1653.05 (C = C ν), 1739.85 (C–CO–C ν), 2925.15 (C–H ν), 2921.22 (C–H ν), 3131.84 (aromatic C–H ν), 3586.75 (O–H ν); ^{1}H NMR δ 7.74 (2H, m, H-3, H-5), 7.69 (1H, m, H-4), 7.52 (2H, m, H-2, H-6), 5.08 (1H, d, J = 12.6 Hz, H-14), 4.24 (2H, t, J = 6.9 Hz, H-8), 4.01 (2H, d, J = 6.63 Hz, H-15), 1.98 (1H, m, H-12), 1.66 (2H, q, J = 9.7, 3.5 Hz, H-9), 1.50 (2H, t, J = 4.7 Hz, H-11), 1.45 (1H, m, H-10), 1.34 (1H, m, H-13), 0.93 (3H, d, J = 6.89 Hz, H-17), 0.87 (3H, d, J = 9.27 Hz, H-16); ^{13}C NMR δ 132.3 (C-1), 130.9 (C-2), 128.8 (C-3), 128.8 (C-4), 128.8 (C-5), 130.9 (C-6), 167.7 (C-7), 65.5 (C-8), 30.5 (C-9), 19.1 (C-10), 38.0 (C-11), 27.7 (C-12), 49.7 (C-13), 101.4 (C-14), 71.7 (C-15), 13.7 (C-16), 18.6 (C-17); ^{1}H-^{1}H COSY and HMBC (Table 1); high resolution electrospray ionization mass spectrometry (HRMS) (ESI) *m/z* calcd. for $C_{17}H_{25}O_4$ 293.1675; found 293.1694 $[M+H]^+$.

13-(Tetrahydro-15β,16α-dimethyl-18-oxo-2H-pyran-14-yl)-10β-methylhept-12(*E*)-enyl benzoate (2)

Brown liquid, UV_{MeOH} λ_{max}: 244 nm (log ε 3.76); TLC (EtOAc/*n*-hexane 1:4 v/v) R_f: 0.65; RP-HPLC (MeOH: ACN, 4:6 v/v) R_t: 11.51 min; IR (ν_{max} in cm^{-1}): 744.55 (mono-subst –C–H δ), 866.07 (aryl –C–H ν), 1462.09 (C–H δ), 1600.97 (C = C ν), 1730.21 (C–CO–C ν), 2855.71 (C–H ν), 2927.08 (C–H ν); ^{1}H NMR δ 7.72 (1H, m, H-3, H-5), 7.70 (1H, m, H-4), 7.52 (1H, m, H-2, H-6), 5.12 (1H, t, J = 11.4 Hz, H-12), 4.31 (2H, t, J = 6.2 Hz, H-8), 4.08 (2H, d, J = 6.8 Hz, H-17), 2.18 (1H, d, J = 4.4 Hz, H-14), 2.06 (2H, m, H-16), 1.98 (2H, d, J = 7.2 Hz, H-11), 1.72 (2H, m, H-9), 1.68 (3H, s, H-21), 1.58 (2H, t, J = 9.06 Hz, H-15), 1.46 (1H, m, H-10), 0.97 (3H, d, J = 10.7 Hz, H-19), 0.88 (3H, d, J = 5.6 Hz, H-22), 0.81 (3H d, J = 6.59 Hz, H-20); ^{13}C NMR δ 133.7 (C-1), 130.9 (C-2), 128.8 (C-3), 128.8 (C-4), 128.8 (C-5), 130.9 (C-6), 167.7 (C-7), 65.5 (C-8), 30.5 (C-9), 19.7 (C-10), 27.9 (C-11), 124.2 (C-12), 144.1 (C-13), 39.7 (C-14), 25.6 (C-15), 29.7 (C-16), 71.2 (C-17), 174.8 (C-18), 13.7 (C-19), 22.6 (C-20), 25.6 (C-21), 16.0 (C-22); ^{1}H-^{1}H COSY and HMBC (Table 1); HRMS (ESI) *m/z* calcd. for $C_{22}H_{30}O_4Na$: 381.2041; found 381.2102 $[M + Na]^+$.

Dihydro-11-((7*E*)-2-hydroxy-8β-methyl-2H-chromen-9-yl)-13-methylpent-12(*E*)-enyl)-17β-methylfuran-19(3*H*)-one (3)

Yellow oil; UV_{MeOH} λ_{max}: 246 nm (log ε 3.92); TLC (EtOAc/*n*-hexane 1:4 v/v) R_f: 0.40; RP-HPLC (H_2O:ACN, 1:1 v/v) R_t: 14.45 min.; IR (ν_{max} in cm^{-1}): 802.41 (aromatic C–H δ), 1087.89 (C–O ν), 1377.22 (C–H ρ), 1558.54 (C = C ν), 1616.40 (C–CO–C ν), 1714.77 (C = O ν), 2922.25 (C–H ν), 3232.80 (aromatic C–H ν), 3486.45, 3551.07 (O–H ν); ^{1}H-NMR: δ 7.19 (1H, d, J = 8.2 Hz, H-5),7.12 (1H, d, J = 9.2 Hz, H-3), 6.77 (1H, t, J = 7.4 Hz, H-4), 6.71 (1H, s, H-7), 5.54 (1H, t, J = 12.6 Hz, H-12), 4.50 (1H, t, J = 11.7 Hz, H-9), 3.87 (1H, m, H-16), 2.32 (2H, d, J = 7.4 Hz, H-18), 2.03 (2H, m, H-15), 1.92 (2H, t, J = 7.1 Hz, H-14), 1.69 (3H, s, H-10), 1.62 (2H, t, J = 6.80 Hz, H-11), 1.52 (1H, m, H-17), 1.30 (3H, s, H-21), 0.88 (3H, d, J = 6.5 Hz, H-20); ^{13}C NMR δ 154.7 (C-1), 157.9 (C-2), 128.1 (C-3), 115.3 (C-4), 127.9 (C-5), 130.0 (C-6), 114.0 (C-7), 133.1 (C-8), 81.7 (C-9), 31.9 (C-10), 38.9 (C-11), 116.9 (C-12), 139.2 (C-13), 33.3 (C-14), 37.7 (C-15), 85.8 (C-16), 29.7 (C-17), 48.7 (C-18), 172.7 (C-19), 14.1 (C-20),

Table 1 ^{1}H-NMR[a], ^{13}C-NMR, ^{1}H-^{1}H COSY, and HMBC assignments of the compounds (in $CDCl_3$) isolated from *R. annamalayana*

	Compound 1		Compound 2		Compound 3	
C. No.	^{13}C	δ^{1}H NMR[b]	^{13}C	δ^{1}H NMR[b]	^{13}C	δ1H NMR[b]
1	132.32	–	133.72	–	154.70	–
2	130.90	7.52 (1H, m)	130.90	7.52 (1H, m)	157.92	–
3	128.84	7.74 (1H, m)	128.84	7.72 (1H, m)	128.13	7.12 (1H, d, 9.2)
4	128.84	7.69 (1H, m)	128.84	7.70 (1H, m)	115.39	6.77 (1H, t, 7.4)
5	128.84	7.74 (1H, m)	128.84	7.72 (1H, m)	127.96	7.19 (1H, d, 8.2)
6	130.90	7.52 (1H, m)	130.90	7.52 (1H, m)	130.02	–
7	167.70	–	167.77	–	114.06	6.71 (1H, s)
8	65.56	4.24 (2H, t, 6.9)	65.57	4.31 (2H t, 6.2)	133.15	–
9	30.58	1.66 (2H, q, 9.7,3.5)	30.58	1.72 (2H, m)	81.75	4.50 (1H, t, 11.7)
10	19.19	1.45 (1H, m)	19.75	1.46 (1H, m)	31.93	1.69 (3H, s)
11	38.05	1.50 (2H, t, 4.7)	27.98	1.98 (2H, d,7.2)	38.97	1.62 (2H, t, 6.80)
12	27.73	1.98 (1H, m)	124.26	5.12 (1H, t, 11.4)	116.95	5.54 (1H, t, 12.6)
13	49.70	1.34 (1H, m)	144.11	–	139.27	–
14	101.42	5.08 (1H, d, 12.6)	–	2.18 (1H, d, 4.4)	–	1.92 (2H, t, 7.1)
15	71.78	4.01 (2H, d, 6.63)	25.69	1.58 (2H, t, 9.06)	–	2.03 (2H, m)
16	13.72	0.87 (3H, d, 9.27)	–	2.06 (2H, m)	85.86	3.87 (1H, m)
17	18.64	0.93 (3H, d, 6.89)	71.21	4.08 (2H, d, 6.8)	29.−70	1.52 (1H, m)
18	–	–	174.89	–	48.76	2.32 (2H, d, 7.4)
19	–	–	13.72	0.97 (3H, d, 10.7)	172.7	–
20	–	–	22.63	0.82 (3H d, 6.59)	14.12	0.88 (3H, d, 6.5)
21	–	–	25.69	1.68 (3H, s)	22.70	1.30 (3H, s)
22	–	–	16.01	0.88 (3H d, 5.6)	–	–

[a]Recorded using Bruker AVANCE III 500 MHz (AV 500) spectrometers

[b]Values in ppm, integration, multiplicity, and coupling constants (J=Hz) are indicated in parentheses. Assignments were made with the aid of the ^{1}H-^{1}H COSY, HSQC, HMBC, and NOESY experiments

22.7 (C-21); ^{1}H-^{1}H COSY and HMBC (Table 1); HRMS (ESI) *m/z* calcd. for $C_{21}H_{27}O_4$ 342.4358; found 342. 4367 $[M+H]^+$.

Biological activities of oxygenated heterocyclic metabolites 1–3

The antioxidant activities of **1–3** were evaluated by using the stable radical, 1, 1-diphenyl-2-picrylhydrazyl (DPPH·) and 2, 2′-azino-bis-3 ethylbenzothiozoline-6-sulfonic acid diammonium salt ($ABTS^{\cdot+}$) assays, as detailed in the earlier works of literature (Lim et al. 2007; Chakraborty and Raola 2017). The anti-inflammatory activities were carried out by using the cyclooxygenase-1, 2 (COX-1 and 2) inhibition assay by 2, 7-dichloroluorescein method and 5-lipoxygenase (5-LOX) inhibition assay, as reported before (Raola and Chakraborty 2017a). The plots of antioxidant and enzyme inhibitory activities were expressed as 50% inhibitory concentration towards oxidants (DPPH. and $ABTS^{\cdot+}$) and pro-inflammatory enzymes COX-1, 2 and 5-LOX (IC_{50}, millimolar or mM). The structural descriptors computed on the ACD Chemsketch (used version 8.0) and ChemDraw Ultra 8.0 platforms were used to corroborate the molecular functionalities with target bioactive properties (Raola and Chakraborty 2017a).

Statistical analysis

Statistical assessments were performed with the Statistical Program for Social Sciences 13.0 (SPSS Inc, Chicago, USA, ver. 13.0) using the triplicate activity results and means were computed for significant differences using analysis of variance studies (ANOVA) at 5% level of significance ($p \leq 0.05$).

Results and discussion

Chemistry

The EtOAc fraction of the leaves of *R. annamalayana* was repeatedly fractionated by column chromatography methods over silica gel and octadecyl silane (reverse-phase). Three (**1–3**) previously undescribed oxygenated heterocyclic metabolites were isolated by chromatographic fractionation, and were characterized as 11-(tetrahydro-14α-hydroxy-13β-methylfuran-12-yl)-10β-methylbutyl benzoate (**1**),

13-(tetrahydro-15β,16α-dimethyl-18-oxo-2*H*-pyran-14-yl)-10β-methylhept-12(*E*)-enyl benzoate (**2**) and dihydro-11-((7*E*)-2-hydroxy-8β-methyl-2*H*-chromen-9-yl)-13-methylpent-12(*E*)-enyl)-17β-methylfuran-19(3*H*)-one (**3**) (Fig. 1) based on spectroscopic methods (MS, NMR).

11-(Tetrahydro-14α-hydroxy-13β-methylfuran-12-yl)-10β-methylbutyl benzoate (**1**) was obtained as a pale yellow liquid by repetitive chromatographic separation. The HR (ESI)MS spectrum exhibited the molecular ion peak at *m/z* 293.1694 (*m/z* 293.1694, calcd. 293.1675 $(M+H)^+$), which is consistent with a molecular formula of $C_{17}H_{24}O_4$ showing six degrees of unsaturation. The ^{13}C NMR in conjugation with distortionless enhancement by polarization transfer (DEPT) (Table 1) displayed the signal arising from one carbonyl at δ 167.70 and carbon signals including three O-attached carbons at δ 65.56, 72.41 and 71.78. The ^{13}C NMR spectrum displayed the carbonyl carbon at δ 167.70 (C-7) and aromatic carbons (δ 132.32, 130.90, 128.84), which displayed close values with the previously reported aryl meroterpenoids (Chakraborty et al. 2016). The UV absorbance at 237 nm was attributed to an aromatic chromophore in **1**. The IR absorption band disclosed the strong stretching vibration bands near 1739 and 1457 cm^{-1} that denoted the occurrence of carbonyl and olefinic groups, respectively. The intense HMBC signal between the proton at δ 7.52 (H-2) with the carbon signal at δ 167.70 (C-7) assigned that the carbonyl group attached to the aromatic ring. A methylene proton at δ 4.24 (H-8) appeared at the downfield place, probably due to the extended conjugation associated with the benzoate framework (Jameel et al. 2015). The ^1H-^1H COSY signals appeared between the protons at δ 4.24 (H-8)/δ 1.66 (H-9)/δ 1.37 (H-10)/δ 1.50 (H-11) and δ 0.87 (H-16) further affirmed the occurrence of 3-methyl butane moiety. In the HMBC data, long-range couplings were recorded between the proton at δ 4.24 (H-8) with δ 167.70 (C-7), δ 30.58 (C-9), δ 19.19 (C-10); δ 1.66 (H-9) /δ 65.56 (C-8), δ 19.19 (C-10); δ 1.45 (H-10)/δ 13.72 (C-16), δ 38.05 (C-11); δ 1.50 (H-11)/ δ 27.73 (C-12), which confirmed the presence of 3-methyl butanoate moiety (Table 1). The ^1H-^1H homo spin system correlations were evident between δ 4.01 (H-15) with δ 1.98 (H-12)/δ 1.26 (H-13)/δ 5.08 (H-14), and δ 0.93 (H-17), which appropriately supported the tetrahydrofuran-2-ol ring. The low-field quaternary carbon (from ^{13}C NMR) signal bearing the carbonyl group (–COO) was attributed to C-7 that was corroborated by the deshielded proton at δ 4.24 (H-8) exhibiting long-range couplings with C-7, which indicated the attachment of isoprene with the aryl network. The oxygenated proton at δ 5.08 (assigned to H-14) was highly deshielded due to the additional hydroxyl group on C-14, and therefore, was attributable to a lactol functional group in the tetrahydrofuran-2-ol ring (Tettamanzi et al. 2007). The occurrence of a hydroxyl group at C-14 was validated by D_2O exchange. The attribution was further corroborated by the low-field shift of the C-14 carbon (δ 101.42). The attachment of tetrahydrofuran-2-ol ring with the butanoate moiety was established by detailed ^1H-^1H COSY, HMBC and HSQC experiments, which confirmed that the monoterpene framework was connected to benzoate moiety at the C-8 position forming 11-(tetrahydro-14α-hydroxy-13β-methylfuran-12-yl)-10β-methylbutyl benzoate. The molecular ion peak at *m/z* 292 $(C_{17}H_{24}O_2)^+$ yielded the fragment ion at *m/z* 277.04 $(C_{22}H_{22}O_4)^{\bullet+}$, which on further fragmentation yielded the butenyl benzoate moiety at *m/z*

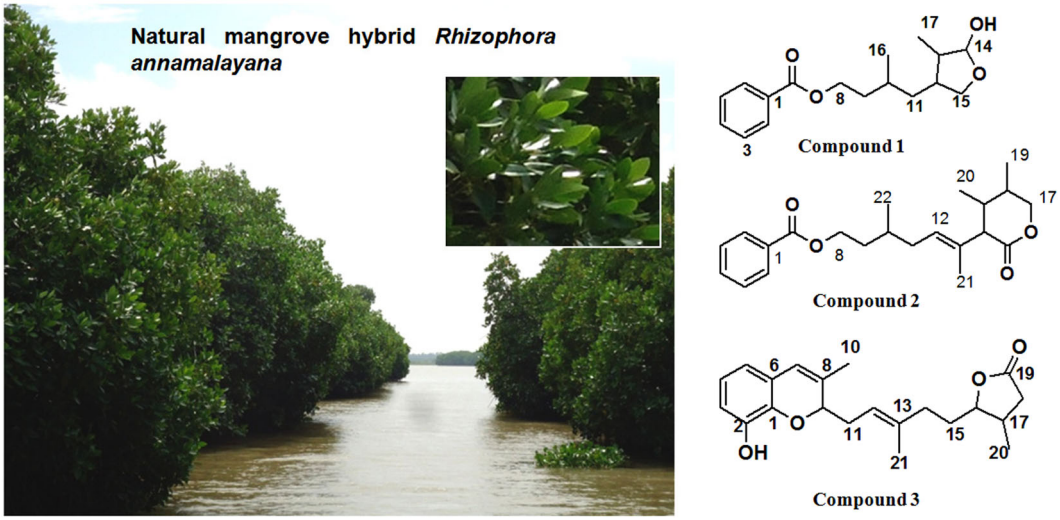

Fig. 1 Natural hybrid mangrove *R. annamalayana* (inset leaves of *R. annamalayana*) and previously undescribed oxygenated heterocyclic metabolites, 11-(tetrahydro-14α-hydroxy-13β-methylfuran-12-yl)-10β-methylbutyl benzoate (**1**), 13-(tetrahydro-15β,16α-dimethyl-18-oxo-2*H*-pyran-14-yl)-10β-methylhept-12(*E*)-enyl benzoate (**2**), and dihydro-11-((7*E*)-2-hydroxy-8β-methyl-2*H*-chromen-9-yl)-13-methylpent-12(*E*)-enyl)-17β-methylfuran-19(3*H*)-one (**3**)

175.07 $(C_{11}H_{12}O_2)^{\bullet+}$. Additional fragments appeared at *m/z* 162 $(C_{10}H_{10}O_2)^{\bullet+}$, *m/z* 147 $(C_9H_8O_2)^{+}$, and *m/z* 149 $(C_9H_{10}O_2)^{\bullet+}$, whereas the latter was recorded as the base peak. The fragment ions at *m/z* 113, 97, and 69 further substantiated the presence of tetrahydrofuranol ring system.

The relative stereochemistries of the chiral centers were ascertained by NOESY experiments (Fig. 2). NOESY correlations were clear between the protons at δ 1.45 (H-10) and δ 1.34 (H-13), which established that these protons were on the same side of the reference plane, and were arbitrarily designated as α-disposed. The NOE signals were apparent within the protons at δ 0.87 (H_3-16)/δ 1.98 (H-12)/0.93 (H_3-17) and δ 5.08 (H-14), which were coplanar, and therefore, were considered to be inclined at the β-plane. The spatial orientation of protons δ 1.34 (H-13) and δ 5.08 (H-14) were determined by the large vicinal couplings 12.6 Hz ($^3J_{13,\ 14}$) of H-14, which indicated that the two protons were axial and in opposite plane. Further, no NOE cross-peaks between these protons confirmed their spatial attributions, thereby assigning the hydroxyl group as equatorially oriented. Based on these combined spectroscopic data, the structure of compound **1** was determined as 11-(tetrahydro-14α-hydroxy-13β-methylfuran-12-yl)-10β-methylbutyl benzoate.

13-(Tetrahydro-15β,16α-dimethyl-18-oxo-2*H*-pyran-14-yl)-10β-methylhept-12(*E*)-enyl benzoate (**2**) was obtained as a brown liquid, and the molecular formula was deduced as $C_{22}H_{30}O_4$ (found 381.2102 $[M + Na]^+$), that indicated eight degrees of unsaturation. The DEPT and ^{13}C NMR spectra revealed the occurrence of 22 carbons comprising four each of methyls, methylenes, and quaternary carbons along with ten methines. The ^{13}C NMR spectrum disclosed highly deshielded signals at δ 133.72 (C-1), δ 130.90 (C-2/C-6), δ 128.84 (C-3/C-4/C-5), together with the corresponding aromatic protons (δ 7.72-7.52), which indicated the presence of aromatic ring (Fig. 3). The deshielded methylene proton at δ 4.31 (H-8) was due to the presence of carbonyl carbon in its vicinity, and this attribution was substantiated by the C–H long-range couplings of H-8 with the carbonyl carbon at C-7. Low-field signal due to the methylene carbon at δ 65.27 (attributed to C-8, $-CH_2$) was in agreement with the presence of an ester group (–COO) (Jameel et al. 2015). The IR absorption bands at 1730 and 1462 cm^{-1} were attributed to the ester carbonyl and olefinic groups, respectively; whereas the UV spectrum displaying λ_{max} absorbance at 244 nm (3.76) recognized the character of an aromatic chromophore. Intense ^1H-^1H COSY signals appeared within δ 4.31 (H-8)/δ 1.72 (H-9)/δ 1.46 (H-10)/δ 0.88 (H-22), and δ 1.98 (H-11)/δ 5.12 (H-12) established the presence of 3-methyl pentane moiety. The long-range HMBC relations between δ 4.31 (H-8)/δ 30.58(C-9); δ 1.72

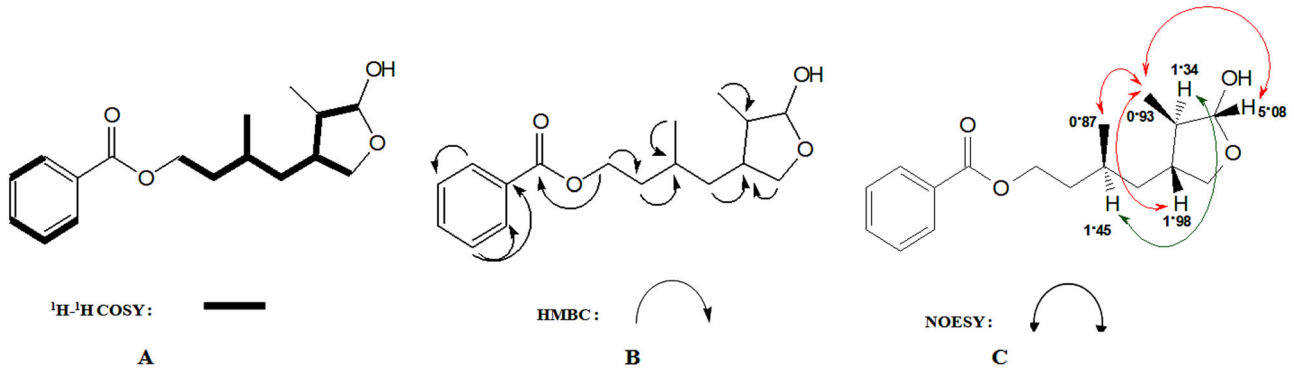

Fig. 2 2D NMR correlations in **1**; **a** ^1H–^1H–COSY couplings (bold face bonds), **b** HMBC couplings (double-barbed arrows) **c** NOESY correlations (indicated as the double-headed arrow)

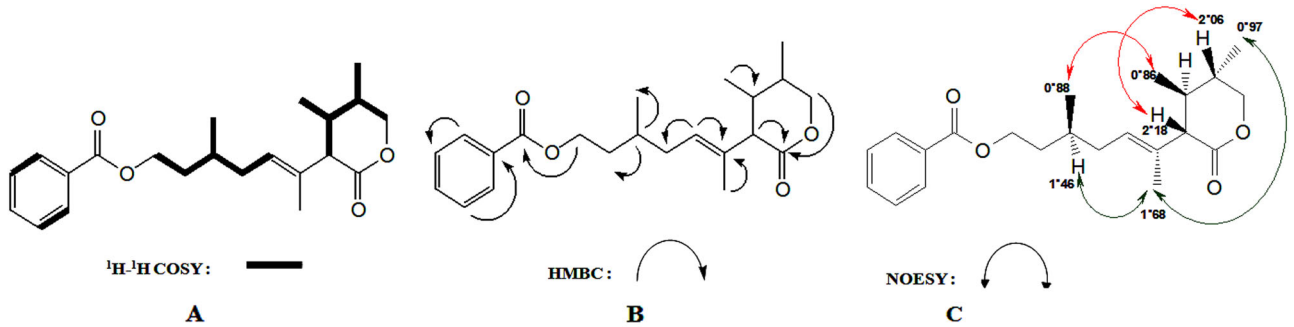

Fig. 3 2D NMR correlations in **2**; **a** ^1H–^1H–COSY couplings (bold face bonds), **b** HMBC couplings (double-barbed arrows) **c** NOESY correlations (indicated as the double-headed arrow)

(H-9)/δ 65.27 (C-8), δ 16.01 (C-22); δ 1.46 (H-10)/δ 16.01 (C-22); δ 1.98 (H-11)/ δ 19.75 (C-10); δ 5.12 (H-12)/δ 27.98 (C-11), δ 144.11 (C-13) revealed the presence of 10β-methylhept-12(*E*)-enyl moiety. The ^{1}H NMR spectrum exhibited one olefinic signal at δ 5.12 (H-12, $J = 11.4$ Hz), which was attached to the carbon C-12 to signify the presence of *trans* orientated trisubstituted double bond. Intense ^{1}H-^{1}H COSY correlations were found at δ 4.08 (H-17)/δ 2.06 (H-16)/δ 0.97 (H_3-19), and δ 2.18 (H-14)/ δ 1.58 (H-15), which supported the partial structure of tetrahydropyran-2-one. Mutual HMBC correlations were evident within δ 2.18 (H-14)/ δ 174.09 (C-18), δ 25.69 (C-15), 144.11 (C-13); δ 4.08 (H-17)/δ 174.09 (C-18), δ 29.70 (C-16), which recognized that the tetrahydropyran-2-one ring was attached to 10β-methylhept-12(*E*)-enyl skeleton. The HMBC correlations at δ 0.86 (H-20)/δ 25.69 (C-15) and δ 0.97 (H-19)/ δ 29.70 (C-16) signified that the two methyl groups (H_3-20 and H_3-19) were located on the pyran-2-one ring to form the tetrahydro-4, 5-dimethylpyran-2-one. The mass fragments at *m/z* 358 $(C_{22}H_{30}O_4)^{\bullet+}$, 122 ($C_7H_5O_2^{\bullet+}$, attributed to benzoate) and 236 {$C_{15}H_{26}O_2^{\bullet+}$, tetrahydrodimethyl-3-(5-methylhept-2-en-2-yl)pyran-2-one} further corroborated the structural assignments. The base peak was recorded at *m/z* 149.05, which was attributed to the ethyl benzoate moiety $(C_9H_9O_2)^{\bullet+}$. Based on these combined spectroscopic data, the structure of compound **2** was determined as 13-(tetrahydro-15β,16α-dimethyl-18-oxo-2*H*-pyran-14-yl)-10β-methylhept-12(*E*)-enyl benzoate.

A previous report of literature reported the occurrence of naturally occurring antioxidative metabolites bearing furanyl benzoate and 2*H*-pyranyl moieties from marine algae *Hypnea musciformis* (Chakraborty et al. 2016). The connections between the carbon and protons, as inferred from the combined HMBC, HSQC, and ^{1}H-^{1}H COSY analyses disclosed the presence of 13-(tetrahydro-15β, 16α-dimethyl-18-oxo-2*H*-pyran-14-yl)-10β-methylhept-12(*E*)-enyl benzoate (Table 1). The H-15 proton resonating as fine triplet displayed large vicinal coupling ($J = 9.06$ Hz) with H-16, and did not show any NOE signal, which recognized that these two protons were axially oriented, and situated in the opposite plane of symmetry. The stereocentres at δ 1.46 (H-10) exhibited NOE cross-peaks with the proton signals at δ 1.58 (H-15), δ 0.97 (H_3-19) along with δ 1.68 (H_3-21), and were, therefore, considered to be in α-plane of the compound. The methine proton attached to C-15 (δ 1.58) did not display NOE interactions with H-16/H-14, which were at the α-referral plane, thereby authenticating that the protons H-16 and H-14 were disposed at the β-plane of the molecule. NOESY correlation between δ 2.18 (H-14)/δ 0.88 (H-22)/δ 0.86 (H-20) and with δ 2.06 (H-16) appropriately inferred that these protons were in proximity and β-disposed.

Dihydro-11-((7*E*)-2-hydroxy-8β-methyl-2*H*-chromen-9-yl)-13-methylpent-12(*E*)-enyl)-17β-methylfuran-19(3*H*)-one (**3**), a previously undescribed 2*H*-chromenol metabolite, was obtained as a yellow oil, and the molecular formula was deduced as $C_{21}H_{26}O_4$ through extensive NMR and HR(ESI) MS experiments (found 342.4367 $[M+H]^+$), indicating nine degrees of unsaturation. This compound exhibited 21 carbon signals with three methyls, four methylenes, eight methines and six quaternary carbons (one oxymethine and two olefins) as inferred from the combined DEPT and ^{13}C NMR experiments. The deshielded carbon signals at δ 154.70 (ascribed to C-1), δ 157.92 (C-2), δ 128.13 (C-3), δ 115.39 (C-4), δ 127.96 (C-5), and δ 130.02 (C-6) represented the aryl carbons, which were typical to the benzene skeleton. The presence of hydroxyl group (at δ 9.76) at C-2 (δ 157.92) led to a significant downfield shift of the C-2 carbon, and this attribution was corroborated by the D_2O exchange experiment. The presence of hydroxyl group was further validated by broad IR stretching vibration at 3551 cm^{-1}. Extensive HMBC correlations were apparent between δ 7.12 (H-3) to δ 157.92 (C-2), δ 115.39 (C-4); δ 6.77 (H-4) to δ 127.96 (C-5), and δ 7.19 (H-5) to δ 130.02 (C-6), which revealed the presence of the phenolic group. The quaternary olefinic signal at δ 133.15 (C-8) and singlet methine at C-7 (HSQC δ 114.06/δ 6.71) represented the presence of trisubstituted olefinic bond. The methine protons at δ 6.71 (H-7) recorded major HMBC cross-peaks with δ 133.15 (attributed to C-8)/δ 81.75 (C-9) and δ 4.50 (H-9)/δ 154.7 (C-1), which revealed the presence of pyran ring attached to the aromatic group at C-1 and C-6 positions forming a bicylcic 2*H*-chromenol moiety in **3**. The methine carbon appeared at δ 81.75 (assigned to C-9, HSQC with δ 4.50), and the attribution was comparable with the reported –CH carbon of 2-(hexaprenylmethyl)-2-methyl-chromenol isolated from the sponge *Ircinia fasciculata* (Venkateswarlu and Reddy 1994).

Two intense ^{1}H-^{1}H COSY signals apparent between δ 4.50 (H-9)/δ 1.62 (H-11)/δ 5.54 (H-12) and δ 1.92 (H-14) and δ 2.03 (H-15)/δ 3.87 (H-16)/δ 1.52(H-17)/δ 2.32 (H-18) inferred the presence of 3-methyl pentene skeleton. Homonuclear ^{1}H-^{1}H COSY correlations were recorded between δ 3.87 (H-16) and δ 1.52 (H-17)/δ 2.32 (H-18), which deduced the partial structure of dihydro-methylfuranone. The methine signal at δ 3.87 (H-16) appeared downfield because of occurrence of carbonyl functional group and the long-range couplings between δ 2.32 (H-18) and δ 172.7 summarized the presence of –C = O(O) group. An intense IR signal at 1714 cm^{-1} supported the presence of carbonyl group.

The 17-methylfuran-19(3*H*)-one moiety was attached at C-15 of 13-methylpent-13-enyl end, which was supported by the long-range C–H correlations from δ 3.87 (H-16) to δ 172.70 (C-19, carbonyl carbon)/δ 29.70 (C-17); δ 2.32 (H-18) to δ 172.70 (C-19); δ 14.12 (H-20) to δ 29.70 (C-17) and δ 1.30 (H-21) to δ 139.27 (C-13), δ 37.70 (C-15).

The ^{1}H NMR showing two singlets at δ 1.69 (HSQC, H-10 with δ 31.93) and δ 1.30 (HSQC, H-21 with δ 22.70) indicated the presence of two methyl groups, which were situated on the olefinic quaternary carbons. These assignments were confirmed by the HMBC relations between δ 1.69 (H-10)/δ 133.15 (C- 8) and δ 1.30 (H-21)/δ 139.27 (C-13). The detailed spectroscopic analysis revealed the presence of 2*H*-chromenol-skeleton (Fig. 4). The mass spectral data disclosed the molecular ion peak at *m/z* 342, which exclude the molecular CO_2 yielding a fragment at *m/z* 298 that was attributed to 3-methyl-2-(3,7-dimethyloct-2-enyl)-2*H*-chromen-8-ol ($C_{20}H_{26}O_2)^{\bullet+}$. An intra-molecular rearrangement of 3,4-dihydro-2*H*-chromen-8-ol ($C_9H_{10}O_2^{\bullet+}$, *m/z*: 148.35) led to the formation of the fragment ion at *m/z* 123.04 (attributed to 3-methylbenzene-1, 2-diol, $C_7H_8O_2^{\bullet+}$) as the base peak.

The geometrical configuration of the double bond at C-12/C-13 of 3-methyl pentene system was designated as *E* (*trans*-), which was deduced from the coupling constant {J = 12.6 Hz (δ 5.54, H-12)}. The NOE correlations between δ 4.50 (H-9) and δ 1.52 (H-17) indicated their proximity and disposition in the identical reference plane (ascribed to α-aligned with reference to the molecular plane of symmetry). Additional NOE signals were recorded between δ 1.69 (H_3-10), δ 3.87 (H-16), δ 0.88 (H-20) and not with H-9/H-17, which apparently indicated that these groups were β-disposed. These combined spectral data substantiated the structure of the compound **3** as dihydro-11-((7*E*)-2-hydroxy-8β-methyl-2*H*-chromen-9-yl)-13-methylpent-12 (*E*)-enyl)-17β-methylfuran-19(3*H*)-one.

Antioxidative and anti-inflammatory activities of oxygenated heterocyclic metabolites 1–3

The oxygenated heterocyclic metabolites isolated from *R. annamalayana* were checked for their antioxidative potentials with respect to the in vitro DPPH (1, 1-diphenyl-2-picrylhydrazyl) and $ABTS^+$ (2, 2′-azino-bis-3 ethylbenzothiozoline-6-sulfonic acid diammonium salt) radical scavenging and inhibitory properties towards pro-inflammatory cyclooxygenase (COX-1 and 2) isoforms and lipoxygenase (5-LOX) enzyme (Table 2). The oxygenated heterocyclic compound bearing 2*H*-chromenyl substituted methylfuran-19(3*H*)-one (compound **3**) displayed significantly greater $DPPH^{\cdot}$ and $ABTS^{\cdot+}$ quenching potential (IC_{50} 2.10 and 2.22 mM, respectively, $p < 0.05$) than that with 14α-hydroxy-13β-methylfuran-12-yl, **1** (IC_{50} 2.77 and 3.22 mM, respectively) and 18-oxo-2*H*-pyran-14-yl, **2** (IC_{50}

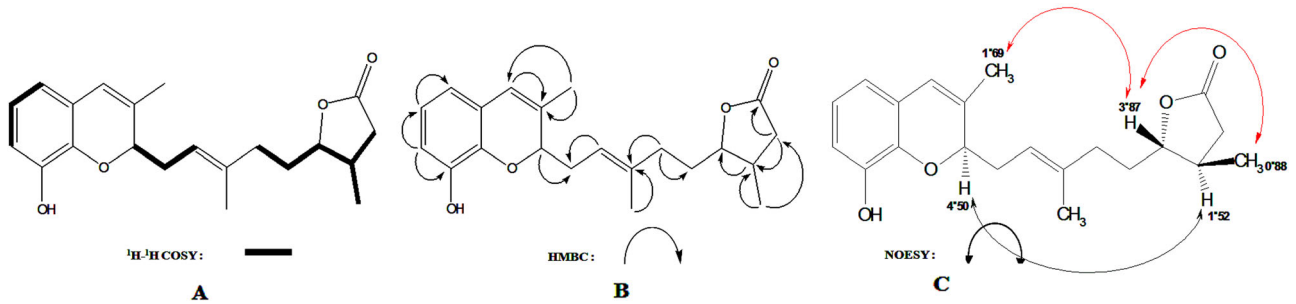

Fig. 4 Two-dimensional NMR correlations in **3**; **a** ^{1}H–^{1}H–COSY couplings (bold face bonds), **b** HMBC couplings (double-barbed arrows) **c** NOESY correlations (indicated as the double-headed arrow)

Table 2 Antioxidative and anti-inflammatory activities of the aryl terpenoids (**1**–**3**) from *R. annamalayana* and commercially available natural and synthetic antioxidants

Bioactivities[a]	IC_{50} (mmol or mM)			
Antioxidative activities	1	2	3	α-tocopherol
$DPPH^{\cdot}$ scavenging	$2.77^c \pm 0.12$	$4.57^d \pm 0.31$	$2.10^c \pm 0.16$	$1.46^c \pm 0.08$
$ABTS^{+\cdot}$ scavenging	$3.22^d \pm 0.16$	$3.12^d \pm 0.19$	$2.22^c \pm 0.14$	$1.69^c \pm 0.12$
Anti-inflammatory activities	1	2	3	Ibuprofen
COX -1 inhibition	$5.81^d \pm 0.24$	$4.99^c \pm 0.28$	$5.31^d \pm 0.19$	$0.19^e \pm 0.08$
COX -2 inhibition	$4.58^d \pm 0.19$	$2.71^c \pm 0.16$	$2.34^c \pm 0.22$	$0.44^e \pm 0.04$
Selectivity index[b]	$4.31^c \pm 0.16$	$5.13^c \pm 0.18$	$6.63^d \pm 0.14$	$2.13^e \pm 0.14$
5-LOX inhibition	$3.35^c \pm 0.15$	$2.57^e \pm 0.11$	$2.16^e \pm 0.09$	$4.51^d \pm 0.18$

[a]The bioactivities were expressed as IC_{50} values (mmol or mM). The samples were analyzed in triplicate (n = 3) and expressed as a mean ± standard deviation. Means followed by the different superscripts (c–e) within the same row indicate significant differences ($p < 0.05$)

[b]Selectivity index has been calculated as the ratio of anti-COX-1(IC_{50}) to that of anti-COX-2 (IC_{50})

4.57 and 3.12 mM, respectively) moieities. Furthermore, compound **3** could act as the antioxidant agent because of significant activity in inhibiting the free radicals (Table 2) and its activity was comparable to the commercially available antioxidant α-tocopherol (IC_{50} 1.5–1.7 mM). Likewise, the compound **3** demonstrated potent inhibition on pro-inflammatory 5-lipoxygenase (IC_{50} 2.16 mM) followed by those displayed by **2** (IC_{50} 2.57 mM), **1** (IC_{50} 3.35 mM), and anti-inflammatory drug ibuprofen (IC_{50} 4.50 mM), in descending order of anti-inflammatory activities. Compound **3** demonstrated significantly greater COX-2 inhibition activity (IC_{50} 2.34 mM) than those displayed by **1** ($IC_{50>}$ 4.5 mM) ($p < 0.05$).

Structure–activity relationship analysis of compounds 1–3

The aryl terpenoids were studied for their structure–activity relationships based upon their molecular descriptors (electronic, hydrophobic, and steric parameters) vis-à-vis their biological activities (Table 3). The hydrophobicity factor was determined from the logarithm of octanol/water coefficient (log P), and was used to predict the effectiveness of drug–target interactions (Raola and Chakraborty 2017a). The log P values of the studied compounds (log P 3-5) were found to be lesser than that of commercially available antioxidant α-tocopherol (log P 9.98), and were within the acceptable limits (log P 2-5) for optimal lipophobic-hydrophilic characteristics leading to greater bioavailability (Ishige et al. 2001). The electronic properties of the studied compounds were directly proportional to radical scavenging and anti-inflammatory potentials (Raola and Chakraborty 2017a). The electronic properties of the studied compounds were determined by the topological polar surface area (tPSA) and polarizability (Pl), which were found to be greater (tPSA > 43; Pl > 32×10^{-24} cm^3, respectively) than those recorded with α-tocopherol (tPSA 29.46) and ibuprofen (tPSA 37.30; Pl 23.76×10^{-24} cm^3, respectively). This apparently indicated the greater electronic interactions of the heterocyclic metabolites described in this study with the reactive radical species and pro-inflammatory enzymes (COX-1, 2, and 5-LOX). The oxygenated heterocyclic metabolites bearing the furanyl backbone (compounds **1** and **3**) with dual cyclooxygenase-2 and 5-lipoxygenase inhibitory potentials exhibited significantly denser electronic properties (tPSA ~55) than **2** (tPSA ~43) due to the presence of terminal tetrahydrofuran-2-ol (in **1**) and furanone rings (in **2**), respectively, along with the aromatic ring. This could further increase the electron resonances leading to the availability of free hydrogens and hydrogen atom transfer (HAT) mediated neutralization of the free radicals. Also, the greater bulkiness of α-tocopherol (MV 462.70 cm^3, MR 135.06 cm^3/mol and Pr 1123 cm^3) than those recorded with the studied compounds (MV < 350 cm^3, MR 80-102 cm^3/mol; Pr > 770 cm^3) explained their ease to neutralize the free radical species. There were reports that the aryl groups and *O*-heterocyclic skeletons (such as chromenol, furananone, tetrahydrofuran-2-ol, and tetrahydro-4, 5-dimethylpyran-2-one moieties) might have a significant role in determining the antioxidant and anti-inflammatory potentials (Shin et al. 2016).

The anti-inflammatory potentials were reported to be directly related to the radical scavenging effects, and therefore, the furanyl heterocyclic metabolites with greater antioxidative activities (**1** and **3**) were found to possess potent anti-inflammatory properties. The aryl terpenoid bearing 2*H*-chromenyl substituted methylfuran-19(3*H*)-one (compound **3**) exhibited greater anti-inflammatory activity, which might be attributed to the electron-rich chromenol and γ-butyrolactone rings (Hegazy et al. 2015). Previous studies recorded that the molecules with a greater number of electronic descriptors, such as hydrophobic centroids, have potential to form hydrogen bonds (hydrogen bonding with acceptors and donors) (Ajay et al. 1998). Hegazy et al. (2015) reported that the substituted aromatic rings have the capacity to interact with the acidic and basic amino acyl residues at the specific binding with sites causing a response to blocks or triggers. The anti-inflammatory selectivity indices (anti-COX-1_{IC50} to anti-COX-2_{IC50}) of the studied compounds were significantly greater (4.3–6.6) than that displayed by ibuprofen (2.13). These previously undescribed metabolites featuring *O*-heterocyclic skeletons with dual cyclooxygenase-2 and 5-lipoxygenase inhibitory potentials from *R. annamalayana* might form potential bioactive leads in medicinal applications.

Conclusions

Bioassay-guided purification of ethyl acetate fraction of the leaves of natural hybrid mangrove *R. annamalayana* yielded three metabolites featuring *O*-furanyl and *O*-pyranyl skeletons. Their structures of these previously undisclosed mangrove metabolites were assigned by comprehensive spectroscopic analyses. The in vitro antioxidative studies revealed the potential of the oxygenated heterocyclic bearing 2*H*-chromenyl substituted methylfuran-19(3*H*)-one (compound **3**) to significantly quench the free radicals, and its activity was comparable to the commercially available antioxidant α-tocopherol. The greater anti-inflammatory

Table 3 The molecular descriptors of aryl terpenoids (**1**–**3**) from *R. annamalayana* and commercially available products

	Electronic		Steric		Hydrophobic	
	tPSA	Pl (X10^{-24} cm^3)	MR (cm^3/mol)	MV (cm^3)	Pr (cm^3)	Log P
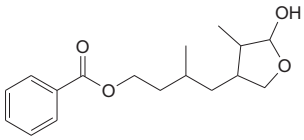 **1**	55.76	32.06	80.87	266.4	671.8	3.55
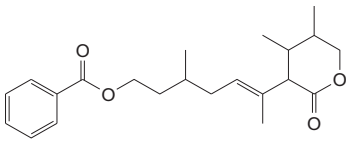 **2**	43.37	40.58	102.38	343.2	841.9	5.17
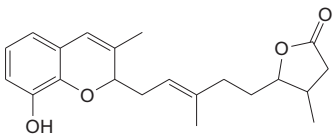 **3**	55.70	38.40	96.88	306.2	766.6	3.79
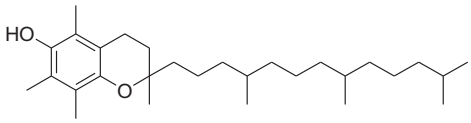 **α-tocopherol**	29.46	53.54	135.06	462.70	1123.00	9.98
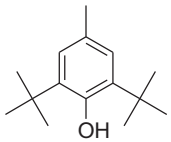 **BHT**	20.23	27.64	69.73	237.50	556.00	5.54
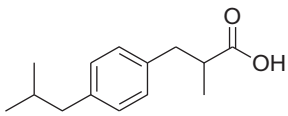 **Ibuprofen**	37.30	23.76	65.8	200.10	499.30	3.50
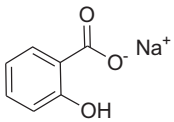 **Na-salicylate**	60.36	13.90	35.06	100.30	284.40	2.27

Pl Polarizability (cm^3/mol), *P* Parachor (cm^3), *tPSA* topological polar surface area based on fragment contributions, *LogP* to calculate *n*-octanol/water partition coefficient, *MR* molar refractivity (cm^3/mol), *MR* to calculate molar refractivity, *MV* molar volume (cm^3)

selectivity indices of the oxygenated heterocyclic analogs than the non-steroidal anti-inflammatory drug showed their higher selectivity towards inhibiting inducible pro-inflammatory cyclooxygenase-2 and 5-lipoxygenase.

Acknowledgements This research was supported by the Indian Council of Agricultural Research (ICAR) Network Project High-Value Compounds (grant no. HVC/ICAR 2012–2017). We thank the Director, Central Marine Fisheries Research Institute for support. Thanks are due to the Head, Marine Biotechnology Division, Central Marine Fisheries Research Institute for facilitating the research activity. VR wishes to acknowledge ICAR, for the award of a scholarship.

Compliance with ethical standards

Conflict of interest The authors declare that they have no conflict of interest.

References

Ajay A, Walters WP, Murcko MA, (1998) Can we learn to distinguish between "drug-like" and "nondrug-like" molecules? J Med Chem 41(18):3314–3324

Alikunhi NM, Kandasamy K, Manoharan C, Subramanian M (2012) Insulin-like antigen of mangrove leaves and its anti-diabetic activity in alloxan-induced diabetic rats. Nat Prod Res 26:1161–1166

Chakraborty K, Joseph D, Joy M, Raola VK (2016) Characterization of substituted aryl meroterpenoids from red seaweed *Hypnea musciformis* as potential antioxidants. Food Chem 212:778–788

Chakraborty K, Raola VK (2017) Two rare antioxidant and anti-inflammatory oleanenes from loop root Asiatic mangrove *Rhizophora mucronata*. Phytochem 135:160–168

Chakraborty K, Raola VK (2018) Previously undescribed benzoxepins with bioactivities against inducible pro-inflammatory cyclooxygenase and lipoxygenase from *Rhizophora annamalayana* Kathir. Nat Prod Res 8:1–9. https://doi.org/10.1080/14786419.2018.1446008

Costa FN, da Silva MD, Borges RM, Leitao GG (2014) Isolation of phenolics from *Rhizophora mangle* by combined counter-current chromatography and gel-filtration. Nat Prod Commun 9:1729–1731

Hegazy MEF, Mohamed TA, Alhammady MA, Shaheen AM, Reda EH, Elshamy AI, Aziz M, Paré PW (2015) Molecular architecture and biomedical leads of terpenes from red sea marine invertebrates. Mar Drugs 13:3154–3181

Ishige K, Schubert D, Sagara Y (2001) Flavonids protect neuronal cells from oxidative stress by three distinct mechanisms. Free Radic Biol Med 30:433–446

Jameel M, Ali A, Ali M (2015) Isolation of antioxidant phytoconstituents from the seeds of *Lens culinaris* Medik. Food Chem 175:358–365

Kathiresan K,(1999) *Rhizophora annamalayana* Kathir (Rhizophoraceae), a new nothospecies from Pichavaram mangrove forest in Southeastern peninsular India Environ Ecol 17(2):500–501

Kusuma S, Kumar PA, Boopalan K, (2011) Potent antimicrobial activity of *Rhizophora mucronata* J Ecobiotechnol. 3:40–41

Lakshmi M, Parani M, Senthilkumar P, Parida A (2002) Molecular phylogeny of mangroves VIII: Analysis of mitochondrial DNA variation for species identification and relationships in Indian mangrove Rhizophoraceae. Wetl Ecol Manag 10(5):355–362

Laskar S, Brahmachari G (2014) Access to biologically relevant diverse chromene heterocycles via multicomponent reactions (MCRs): Recent advances. J Org Biomol Chem 2:1–50

Lim YY, Lim TT, Tee JJ (2007) Antioxidant properties of several tropical fruits: A comparative study. Food Chem 103:1003–1008

Martins JN, Figueiredo FS, Martins GR, Leitão GG, Costa FN (2017) Diterpenes and a new benzaldehyde from the mangrove plant *Rhizophora mangle*. Rev Bras Farmacogn 27(2):175–178

Moovendhan M, Ramasubburayan R, Vairamani S, Shanmugam A, Palavesam A, Immanuel G (2015) Antibiotic efficacy and characterization of mangrove metabolites against UTI Microbes. J Herbs Spices Med. Plants 21:129–139

Nebula M, Harisankar HS, Chandramohanakumar N (2013) Metabolites and bioactivities of Rhizophoraceae mangroves. Nat Prod Bioprospect 3:207–232

Parani M, Lakshmi M, Elango S, Ram N, Anuratha CS, Parida A (1997) Molecular phylogeny of mangroves II. Intra and interspecific variation in *Avicennia* revealed by RAPD and RFLP markers. Genome 40(4):487–495

Ragavan P, Jayaraj RSC, Saxena A, Mohan PM, Ravichandran K (2015) Taxonomical identity of *Rhizophora×annamalayana* Kathir and *Rhizophora×lamarckii* Montrouz (Rhizophoraceae) in the Andaman and Nicobar Islands, India. Taiwania 60:183–193

Raola VK, Chakraborty K (2017a) Two rare antioxidative prenylated terpenoids from loop-root Asiatic mangrove *Rhizophora mucronata* (Family Rhizophoraceae) and their activity against pro-inflammatory cyclooxygenases and lipoxidase. Nat Prod Res 31(4):418–427

Raola VK, Chakraborty K (2017b) Biogenic guaianolide-type sesquiterpene lactones with antioxidative and anti-inflammatory properties from natural mangrove hybrid *Rhizophora annamalayana*. Nat Prod Res 31(23):2719–2729

Rocha-Santos T, Duarte A (2014) Introduction to the analysis of bioactive compounds in marine samples. In: Barcelo D (ed). Comprehensive analytical chemistry: Analysis of marine samples in search of bioactive compounds. vol 65, 1st edn, Elsevier, Portugal, pp. 312.

Rohini RM, Das AK (2010) Triterpenoids from the stem bark of *Rhizophora mucronata*. Nat Prod Res 24:197–202

Shin HJ, Pil GB, Heo SJ, Lee HS, Lee JS, Lee YJ, Lee J, Won HS, (2016) Anti-Inflammatory activity of tanzawaic acid derivatives from a marine-derived fungus *Penicillium steckii* 108YD142 Mar Drugs 14:14

Tettamanzi MC, Biurrun FN, Cirigliano AM (2007) A new antifeedant withanolide from *Jaborosa lanigera*. Z Naturforsch 62:573–576

Venkateswarlu Y, Reddy MVR (1994) Three new heptaprenylhydroquinone derivatives from the sponge *Ircinia fasciculata*. J Nat Prod 57:1286–1289

Wang J, Xiang W, Guo Y (2004) Agallochaols A and B, two new diterpenes from the Chinese mangrove *Excoecaria agallocha*. Helv Chim Acta 87:2829–2833

Wang J, Xiang W, Guo Y (2005) Secoatisane- and isopimarane-tpye diterpenoids from the Chinese mangrove *Excoecaria agallocha* L. Helv Chim Acta 88:979–985